# Thermal Contact Conductance at Low Contact Pressures

F. Milanez[*], M. M. Yovanovich[†] and M. B. H. Mantelli[‡]

[*‡]Satellite Thermal Control Group
Federal University of Santa Catarina
Florianopolis, SC, Brazil

[†]Microelectronics Heat Transfer Laboratory
University of Waterloo
Waterloo, ON, Canada

**36th AIAA Thermophysics Conference**
23-26 June 2003 / Orlando, FL

For permission to copy or to republish, contact the American Institute of Aeronautics and Astronautics, 1801 Alexander Bell Drive, Suite 500, Reston, VA, 20191-4344.

# THERMAL CONTACT CONDUCTANCE AT LOW CONTACT PRESSURES

**F. H. Milanez** [*]
**M. M. Yovanovich** [†]
**M. B. H. Mantelli** [‡]

[*‡] Satellite Thermal Control Group
Department of Mechanical Engineering
Federal University of Santa Catarina
Florianopolis, SC, Brazil, 88040-900

[†]Microelectronics Heat Transfer Laboratory
Department of Mechanical Engineering
University of Waterloo
Waterloo, ON, Canada, N2L 3G1

## ABSTRACT

This work presents new correlations for the Truncated Gaussian-TG thermal contact conductance model during first loading. The TG model is also incorporated into an existing model for the hysteresis effect of thermal contact conductance and into an existing plastic contact pressure model. The models are compared against new experimental data collected at very low contact pressures. The comparison between the models and the data show that the fully Gaussian model underpredicts data at low contact pressures, as already extensively reported in the literature. The first-loading TG model predicts the experiments very well over the entire range of the contact pressures tested. The hysteresis effect model proved to be accurate only for contact pressure above 400 kPa, in general. The TG model requires a surface roughness parameter, the level of truncation of the probability density function of surface heights $z_{trunc}$, that can not be obtained accurately from ordinary surface profilometry. The most accurate and straightforward way to estimate this surface geometry parameter is from thermal tests.

## NOMENCLATURE

| | |
|---|---|
| $a$ | mean contact spot radius [m] |
| $A$ | area [$m^2$] |
| $c_1$ | Vickers microhardness correlation coeff. [Pa] |
| $c_2$ | Vickers microhardness correlation coeff. [ - ] |
| $d_v$ | Vickers test indentation diagonal [$\mu$m] |
| $h_c$ | contact conductance [W/m² °C] |
| $H$ | micro-hardness [Pa] |
| $k$ | thermal conductivity [W/m°C] |
| $k_s$ | $=2k_A k_B/(k_A+k_B)$ [W/m°C] |
| $m$ | combined mean absolute slope [rad], $=\sqrt{m_A^2 + m_B^2}$ |
| $n$ | density of contact spots [$m^{-2}$] |
| Ni | Nickel |
| $p$ | interpolation index [ - ] |
| $P$ | contact pressure [Pa] |
| $q$ | heat flux [W/m²] |
| SS | stainless steel |
| $T$ | temperature [°C] |
| $TG$ | Truncated Gaussian |
| $X$ | dummy variable [ - ] (see Eqs. 16, 17 and 18) |
| $z_{trunc}$ | truncation level of the surface heights pdf [ - ] |
| $Z$ | limit of $X$ [ - ] |

Greek Symbols:

| | |
|---|---|
| $\Delta T$ | temperature drop [°C] |
| $\lambda$ | dimensionless mean separation gap |
| $\sigma$ | combined RMS roughness [m], $=\sqrt{\sigma_A^2 + \sigma_B^2}$ |

Subscripts:

| | |
|---|---|
| $a$ | apparent |
| A,B | contacting bodies |
| $c$ | contact |
| $v$ | Vickers micro-hardness test |
| $r$ | real |
| $m$ | mean |
| $max$ | at maximum pressure |

## INTRODUCTION

Heat transfer across the interface between two solids has been the subject of study of various researchers in the last decades. Contact heat transfer has many applications in engineering, such as ball bearings, microelectronic chips and nuclear fuel heat dissipation. Thermal contact resistance is also important in spacecraft applications. The electronic modules necessary for spacecraft missions are

[*] Research assistant, milanez@labsolar.ufsc.br
[†]Distinguished Professor Emeritus, Fellow AIAA, mmyov@mhtlab.uwaterloo.ca.
[‡]Professor, Department of Mechanical Engineering, Member AIAA, marcia@labsolar.ufsc.br.

attached to the spacecraft structure generally by means of bolted joints or other clamping devices. Thermal contact resistances appear at these interfaces and need to be quantified.

There are several theoretical and experimental studies on the thermal contact conductance in the open literature, specially for the contact between conforming rough surfaces. One of the most accepted theoretical thermal contact conductance models was developed by Cooper, Mikic and Yovanovich-CMY[1] for isotropic surfaces deforming plastically. Other models have been developed based on the CMY model, such as the Mikic[2] unloading model, among many others. Sridhar and Yovanovich[3] made an extensive review of the most frequently used thermal contact conductance models. They compared the models against experimental data collected by other researchers and concluded that the CMY based models are the easiest to use and are very accurate, especially when the surfaces are subjected to relatively high contact pressures. At low contact pressures, the models systematically underestimate experimental data.

Recently, Milanez et al.[4] proposed an explanation for this unexpected behavior of the thermal contact conductance at low contact pressures. According to these authors, the reason why the models underpredict the experiments at low contact pressures is the truncation of the highest contacting asperities. The CMY based models, as well as many other theoretical models, assume that the height distribution of the asperities that constitute a real surface is Gaussian. Milanez et al.[4] showed that this hypothesis is valid only up to some extent: real surfaces may have Gaussian height distribution up to 4.5 times the RMS roughness ($\sigma$), approximately, but they generally do not have asperities above $4.5\sigma$. In other words, the highest asperities are shorter than predicted by the Gaussian model. Since the highest asperities are shorter than expected, the mean separation gap between contacting surfaces at low contact loads is smaller than predicted. As a consequence, the contact conductance is larger than predicted. As the contact pressure increases, more and more asperities that are not truncated come into contact. The effect of the few truncated asperities then becomes negligible, and the Gaussian model is accurate at higher contact pressures.

Song[5] and Milanez et al.[4] proposed the basis for a new theoretical model for thermal contact conductance at low contact pressures: the Truncated Gaussian-TG model. This new model, which is also based on the CMY model, is developed in more details here. A simple correlation is provided for this model. The TG model is also incorporated here into the model proposed by Mikic[2] to predict the hysteresis effect of contact conductance and into the Song and Yovanovich[6] model for the plastic contact hardness. The models are then compared against new thermal contact conductance data carefully collected under very light contact pressures during two loading/unloading cycles of contact load.

## REVIEW OF THERMAL CONTACT CONDUCTANCE MODELS

Real surfaces obtained by the actual machining processes present deviations from their idealized geometry. When real surfaces are analyzed in a microscopic scale, roughness and waviness can be observed. When two bodies are put into contact, they will touch each other only at their highest asperities. These asperities are deformed, generating small contact spots. The real contact area is only a very small fraction of the apparent area. In the remaining portion of the apparent contact area the two surfaces are separated by small gaps.

The heat transfer through the interface between two solids can take place by three different mechanisms: conduction through the contact spots, radiation through the gap between the solids and conduction through gas or fluid that may fill the gap. These three mechanisms are generally treated separately, and the thermal conductance of the joint is the summation of the three parts: contact, radiation and gap conductances. There are numerous theoretical models available in the literature to predict these heat transfer mechanisms. In this work, a vacuum environment is considered, which means that the gap conductance is negligible. Also, small temperature differences and relatively low temperature levels are considered, meaning that radiation can also be neglected. Therefore, in this work, the thermal conductance of the interface is a function of the heat flow through the contact spots only.

The existing thermal contact conductance models can be classified according to the deformation mode assumed for the contacting asperities: elastic, plastic or elastoplastic. Under plastic deformation, the asperities are permanently deformed during loading and do not recover their original shape after the surfaces are pulled apart. Under elastic deformation, as the surfaces are pulled apart the asperities recover the original shape. For the elastoplastic case, some intermediate behavior between fully plastic and fully elastic deformation is observed.

The elastic models predict exactly the same behavior for thermal contact conductance during ascending and descending levels of contact pressure. On the other hand, the plastic models were developed for the first loading between the contacting surfaces

only. During unloading, the contact spots are larger than predicted by the plastic models because of the permanent deformation of the asperities during first loading. As a consequence, the thermal contact conductance in descending pressure levels is greater than during the first loading. This phenomenon is known as hysteresis effect of contact conductance.

The CMY based models will be employed here because a comparative study presented by Sridhar and Yovanovich[3] showed that these models are suitable to predict SS 304 and Ni 200 contacts, which are the materials employed in the experimental study developed here. These models can be divided into three sub-models: thermal, geometrical and deformation models. The thermal model predicts the thermal contact conductance for a given set of contact parameters, which are the shape, mean size and number of contact spots. These contact parameters are obtained using a particular deformation model and a geometry model. Cooper et al.[1] employed the Gaussian model for the surface asperity height distribution and assumed random distribution of asperities over the apparent contact area. In these models it is also assumed that the surface roughnesses are isotropic and therefore the contact spots are circular in shape.

Thermal model

According to the Cooper et al.[1] thermal model, the thermal contact conductance between conforming isotropic rough surfaces as a function of the contact parameters is given by:

$$h_c = \frac{2k_s n a}{\left(1-\sqrt{A_r/A_a}\right)^{3/2}} \tag{1}$$

where $n$ is the density of contact spots per unit apparent area, $a$ is the mean contact spot radius, $A_r/A_a$ is the real-to-apparent contact area ratio and $k_s=2k_Ak_B/(k_A+k_B)$ is the harmonic mean of the thermal conductivities of the two bodies. The contact parameters $a$, $n$ and $A_r/A_a$ are obtained from the surface geometry and the deformation models. The contact parameters assuming plastic deformation during the first loading of contact pressure and for the fully Gaussian and the Truncated Gaussian geometry models will be presented now.

Fully Gaussian geometry model

By assuming that the distributions of the surface heights and slopes are independent from each other and follow the Gaussian distribution, as well as assuming that the surfaces undergo plastic deformation, Cooper et al.[1] presented an analysis to derive expressions for the contact parameters for the first loading of the contact pressure. Yovanovich[7] presented the contact parameter expressions for the isotropic plastic model in a more convenient form:

$$n = \frac{1}{16}\left(\frac{m}{\sigma}\right)^2 \frac{\exp\left(-\lambda^2\right)}{\operatorname{erfc}\left(\lambda/\sqrt{2}\right)} \tag{2}$$

$$a = \sqrt{\frac{8}{\pi}}\frac{\sigma}{m}\exp\left(\lambda^2/2\right)\operatorname{erfc}\left(\lambda/\sqrt{2}\right) \tag{3}$$

$$\lambda = \sqrt{2}\ \operatorname{erfc}^{-1}\left(2\frac{A_r}{A_a}\right) \tag{4}$$

$$\frac{A_r}{A_a} = \frac{P}{H_c} \tag{5}$$

where $\sigma$ and $m$ are the combined RMS roughness and mean absolute slope of the surface asperities, which are geometrical parameters that must be obtained from surface profilometry. The apparent contact pressure is $P$ and the contact plastic hardness is $H_c$. Substituting the expressions for the contact parameters (Eqs. 2 to 5) into the thermal model (Eq. 1), one obtains:

$$C_c \equiv \frac{h_c}{k_s}\frac{\sigma}{m} = \frac{\sqrt{2}}{4\sqrt{\pi}}\frac{\exp\left(-\lambda^2/2\right)}{\left(1-\sqrt{P/H_c}\right)^{3/2}} \tag{6}$$

Yovanovich[7], presented the following simple correlation for Eq. (6):

$$\frac{h_c\sigma}{k_s m} = 1.25\left(\frac{P}{H_c}\right)^{0.95} \tag{7}$$

Truncated Gaussian (TG) geometry model

Milanez et al.[4] proposed new expressions for the contact parameters according to the Truncated Gaussian-TG model. The TG model assumes that the distribution of surface heights follow the Gaussian distribution up to a defined value $z_{trunc}$, which is the truncation level. According to the TG model, there are no asperities higher than the truncation level, i. e., $z \le z_{trunc}$. The contact parameters according to the TG model are given by:

$$a = \sqrt{1-\frac{\operatorname{erfc}\left(z_{trunc}/\sqrt{2}\right)}{\operatorname{erfc}\left(\lambda/\sqrt{2}\right)}}\frac{2\sqrt{2}}{\sqrt{\pi}}\frac{\sigma}{m}\exp\left(\frac{\lambda^2}{2}\right)\operatorname{erfc}\left(\frac{\lambda}{\sqrt{2}}\right) \tag{8}$$

where:

$$\lambda = \sqrt{2}\ \operatorname{erfc}^{-1}\left[2\frac{P}{H_c} + \operatorname{erfc}\left(\frac{z_{trunc}}{\sqrt{2}}\right)\right] \tag{9}$$

The density of contact spots $n$ and the real-to-apparent area ratio $A_r/A_a$ are computed using the same expressions as for the fully Gaussian model, Eqs. (2) and (5). Substituting Eqs. (2), (5), (8) and (9) into the thermal model, Eq. (1), one gets the expression for the thermal contact conductance

according to the TG geometry model. Since the final expression is difficult to manipulate, the present authors developed the following correlation that gives a maximum difference of 4% compared with the exact expression:

$$h_c = 1.25\frac{m}{\sigma}k_s\left(\frac{P}{H_c}\right)^{0.95}\left[1+\frac{1}{f}\right]^{0.9289}\sqrt{1-\frac{1}{1+f}} \quad (10)$$

where:

$$f = \frac{P}{H_c}\sqrt{2\pi}\, z_{trunc}\, \exp\left(\frac{z_{trunc}^2}{2}\right) \quad (11)$$

is a function that takes into account for the truncation effect on the thermal contact conductance. In the limiting case where $z_{trunc}\rightarrow\infty$, i. e., the distribution of surface heights is fully Gaussian, $f\rightarrow\infty$ and Eq. (10) gives exactly the same correlation as proposed by Yovanovich[7] for fully Gaussian distribution of surface heights, Eq. (7). Therefore, the CMY model is the limiting case of the TG model when the surface height distribution is not truncated. In practical applications, when $f > 40$ the difference between the fully Gaussian, Eq. (7), and the TG, Eq. (10), models is less than 1%.

Plastic contact hardness

An important parameter appearing in the models presented so far is the dimensionless plastic contact pressure $P/H_c$. Song and Yovanovich[6] proposed a model to predict this parameter. Assuming a fully Gaussian distribution for the surfaces heights, they developed the following model:

$$\left.\frac{P}{H_c}\right|_{Gaussian} = \left[\frac{P}{c_1(1.62\sigma/m)^{c_2}}\right]^{\frac{1}{1+0.071c_2}} \quad (12)$$

where $c_1$ and $c_2$ are the Vickers micro-hardness correlation coefficients of the softer of the two contacting surfaces. In this expression, $\sigma$ must be in micrometers. They are obtained by performing micro-hardness tests for several indentation loads (between 10 and 200 grams) and then correlating the measured Vickers hardness values ($H_v$) to the respective diagonal of lengths ($d_v$) of the square impressions left by the indenter in the following form:

$$H_v = c_1(d_v)^{c_2} \quad (13)$$

Employing the same procedure as Song and Yovanovich[6], the present authors developed the following correlation for the dimensionless contact pressure $P/H_c$, according to the Truncated Gaussian model:

$$\frac{P}{H_c} = \left[\left(\left.\frac{P}{H_c}\right|_{Gaussian}\right)^{-p} + \left(\left.\frac{P}{H_c}\right|_{TG}\right)^{-p}\right]^{-\frac{1}{p}} \quad (14)$$

where:

$$\left.\frac{P}{H_c}\right|_{TG} = \left\{\frac{P}{c_1(2.178\sigma/m)^{c_2}}\left[erfc\left(\frac{z_{trunc}}{\sqrt{2}}\right)\right]^{0.4289c_2}\right\}^{\frac{1}{1+0.5c_2}} \quad (15)$$

and $p = 3.9 + 52\exp(10\,c_2)$. In the limiting case where $z_{trunc}\rightarrow\infty$, Eq. (15) goes to zero and Eq. (14) shows that $P/H_c$ is equal to Eq. (12), which was developed for Gaussian surfaces, as already mentioned. In this work, Eq. (14) is used in order to compute the dimensionless contact pressure $P/H_c$, which is an input to the TG thermal contact conductance model, Eqs. (10) and (11).

Hysteresis effect model according to the TG geometry model

The models presented so far are valid only during the first loading of contact pressure, when the surfaces are deformed plastically. If now the contacting pair is pressed against each other up to a maximum contact pressure $P_{max}$ and then the contact load is decreased to a new contact pressure $P_1$ so that $P_1 < P_{max}$, the thermal contact conductance at $P_1$ is larger than the value obtained at $P_1$ during first loading due to the hysteresis effect of thermal contact conductance, as mentioned before. Mikic[2] proposed an explanation for this phenomenon as follows. During first loading, the asperities deform plastically up to the maximum contact pressure $P_{max}$, and then, during subsequent unloading, the asperities recover part of the deformation elastically. But not all the plastic deformation is recovered during unloading and, as a consequence, the real contact area during unloading is larger than during first loading for the same contact pressure. Therefore the contact conductance during unloading is larger than during loading. If the surfaces are then re-loaded, the deformation is elastic and reversible, i. e., it is possible to return to the same value of contact conductance at $P_{max}$ as during the first loading. Mikic[2] proposed an analytical model for the contact parameters during unloading for surfaces undergoing plastic deformation during first loading. The present authors adapted the unloading model proposed by Mikic[2] to incorporate the Truncated Gaussian geometry model. The set of equations for the contact parameters during unloading, taking into account for the Truncated Gaussian geometry model are presented in Table 1.

**Table 1** – Contact parameters during unloading

$$\frac{P}{H_{\max}} = \frac{\dfrac{4\pi}{(2\pi)^{3/2}} \int_Z^{\infty} \left(\lambda_{\max} + X^2\right) \exp\left[-\left(\lambda_{\max} + X^2\right)^2 / 2\right] X^3 \left(1 - \dfrac{Z}{X}\right)^{3/2} dX}{1 + \dfrac{\dfrac{1}{2}\operatorname{erfc}\left(\dfrac{z_{trunc}}{\sqrt{2}}\right)}{\dfrac{4\pi}{(2\pi)^{3/2}} \int_Z^{\infty} \left(\lambda_{\max} + X^2\right) \exp\left[-\left(\lambda_{\max} + X^2\right)^2 / 2\right] X^3 \left(1 - \dfrac{Z}{X}\right) dX - \dfrac{1}{2}\operatorname{erfc}\left(\dfrac{z_{trunc}}{\sqrt{2}}\right)}} \tag{16}$$

$$\frac{A_r}{A_a} = \frac{4\pi}{(2\pi)^{3/2}} \int_Z^{\infty} \left(\lambda_{\max} + X^2\right) \exp\left[-\left(\lambda_{\max} + X^2\right)^2 / 2\right] X^3 \left(1 - \frac{Z}{X}\right) dX - \frac{1}{2}\operatorname{erfc}\left(\frac{z_{trunc}}{\sqrt{2}}\right) \tag{17}$$

$$n = n_{\max} - \frac{1}{4} \int_0^Z \frac{\exp\left[-\left(\lambda_{\max} + X^2\right)^2\right]}{\operatorname{erfc}\left[\left(\lambda_{\max} + X^2\right)/\sqrt{2}\right]} \left\{ \lambda_{\max} - \frac{1}{\sqrt{2\pi}} \frac{\exp\left[-\left(\lambda_{\max} + X^2\right)^2 / 2\right]}{\operatorname{erfc}\left[\left(\lambda_{\max} + X^2\right)/\sqrt{2}\right]} \right\} X \, dX \tag{18}$$

$$a = \sqrt{\frac{A_r}{A_a} \frac{1}{n\pi}} \tag{19}$$

In Table 1, $H_{max}$ is the plastic hardness, $\lambda_{max}$ is the mean separation gap and $n_{max}$ is the number of contact spots, all evaluated at the maximum contact pressure $P_{max}$. These parameters are computed using Eqs. (14), (9) and (2), respectively. The model requires an iterative procedure in order to compute the contact parameters. For a given contact pressure $P < P_{max}$, Eq. (16) is numerically solved for $Z$. Then $Z$ is substituted into Eqs. (17) to (19) in order to compute the contact parameters $A_r/A_a$, $n$ and $a$. The contact parameters are finally substituted into Eq. (1) to obtain the contact conductance $h_c$. Eqs. (16) to (19) can reproduce the fully Gaussian model, as proposed by Mikic[2], as well. When $z_{trunc} \to \infty$ ($z_{trunc}$=5 in practical applications) Eqs. (16) to (19) give exactly the same expressions as the fully Gaussian model.

## EXPERIMENTAL STUDY

The experimental study consisted of measuring the thermal contact conductance between two SS 304 or two Ni 200 specimens under vacuum environment. The two specimens are nominally flat. One of the contacting specimens is smooth (lapped) and the other is rough (ground or bead blasted). Three roughness levels of each metal were tested.

### Experimental Set-up

The experimental set-up is shown in Fig. 1. It consists of a cold plate, a test column, a load cell, an electrical heater and a loading mechanism. The cold plate is a hollow copper cylinder filled with glycol at a controlled temperature. The test column, consisting of two test specimens and one ARMCO iron flux-meter, is placed on the cold plate. The electrical heater is placed on the top of the ARMCO flux-meter and can dissipate up to 60 W. Radiation heat losses from the test column are minimized by surrounding the column with a polished aluminum tube.

The load is applied to the test column by means of an articulated arm. The loading arm is connected to a shaft. The extremity of the shaft is external to the vacuum chamber and is connected to a nut as shown in Fig. 1. The nut can be rotated by means of a wrench, applying or releasing load to the test column. Between the nut and the chamber base there is a spring that is designed to absorb the thermal expansion of the testing column, avoiding contact pressure variations as a function of temperature variations of the test column during heating. The contact load is read by means of a calibrated load cell assembled in series with the test column and connected to the data acquisition system.

Six #36 type T thermocouples are attached to each test specimen and to the ARMCO flux-meter. The thermocouples are positioned 5 mm apart from each other along the longitudinal direction. The thermocouple voltages are read by a data acquisition system controlled by a personal computer. Every five

seconds, the computer receives the 18 thermocouple voltages, as well as the load cell signal and the electrical heater voltage. The thermocouple signals are converted to temperature values and the load cell signal is converted to load, using pre-defined correlations. The computational code uses a least square method to find the best linear fit for the temperature distribution inside each test specimen and inside the ARMCO flux-meter. The heat fluxes of each sample are obtained by multiplying the slope of the temperature distributions by the respective conductivities. The conductivities of the ARMCO Iron flux-meter and of the SS 304 and Ni 200 test specimens are computed using the following correlations:

$$k_{\mathrm{ARMCO}} = 74.6 - 0.069\,T \quad 0 < T < 100°C \quad (20)$$

$$k_{\mathrm{SS304}} = 17.7 + 0.028\,T \quad 4 < T < 90°C \quad (21)$$

$$k_{\mathrm{Ni200}} = 90.27 - 0.18\,T \quad 5 < T < 90°\mathrm{C} \quad (22)$$

The correlation for the ARMCO Iron was obtained using the tabulated values available in the literature.[9] The correlations for the SS 304 and for the Ni 200 were obtained in a previous conductivity test. The conductivity test employed the same experimental set-up described here. One SS 304 (or Ni 200) specimen was placed between two ARMCO flux-meters. The conductivity of the sample was found by dividing the average heat flux of the two ARMCO flux-meters by the slope of the temperature distribution inside the specimen. This conductivity value was assigned to the mean temperature of the specimen. The tests were performed at various mean temperature levels of the specimens. The measured values of conductivity were then correlated to the respective temperatures, as presented in Eqs. (21) and (22).

Test Procedure

The test pair, consisting of a flat lapped specimen and a bead blasted surface, was assembled inside the vacuum chamber with no load applied by the loading arm. Therefore, the first contact pressure level (15.8 kPa for SS 304 and 16.2 kPa for Ni 200) is determined by the dead weights of the upper specimen, flux-meter and electric heater. The chamber was closed and vacuum was drawn using a mechanical pump connected in series with a diffusion punp. The vacuum inside the chamber was $10^{-6}$ Torr. The electrical heater was turned "on" and the system was left for at least 16 hours to achieve steady state.

The thermal contact conductance was computed by means of the following expression:

$$h_c = \frac{q}{\Delta T} \quad (23)$$

where $q$ is the average of the heat fluxes inside the two contacting specimens. The temperature drop $\Delta T$, appearing in Eq. (23), is computed by extrapolating the temperature profiles of each contacting specimen to the interface.

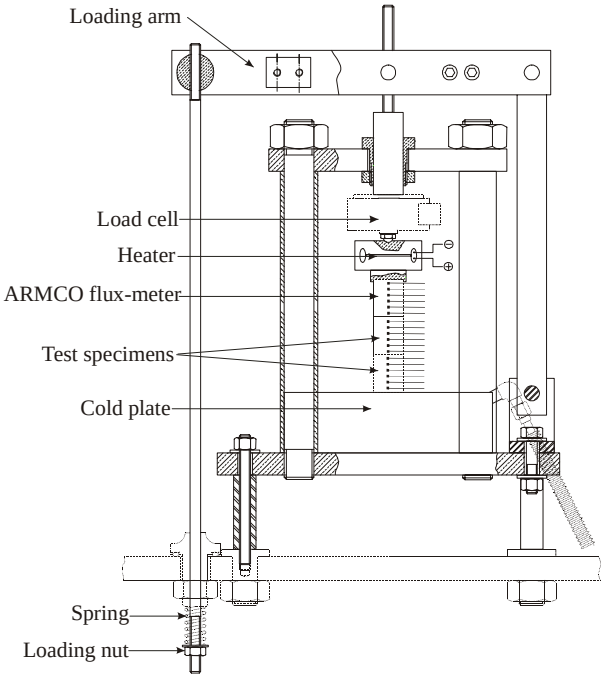


**Figure 1 -** Experimental set-up

This procedure was repeated for each contact pressure level tested. The pressure levels varied from approximatelly 16 kPa to 3000 kPa in both ascending and descending levels. Two loading/unloading cycles were measured for each pair.

For the lightest contact pressure tested the steady state was achieved after 12 hours. As the contact pressure level was increased, the time spent to achieve steady state became smaller. For the maximum pressure tested, approximately 3000 kPa the time required to achieve steady state was less than 2 hours. The system was considered to be in steady state when the thermal contact conductance between the specimens did not vary more than 1% in 1 hour. As the contact pressure was increased between each pressure step, the power level of the electrical heater was increased in order to maintain a reasonable temperature drop between the samples.

Uncertainty Analysis

The total uncertainty in thermal conductivity estimation using Eqs. (21) and (22) are 5.8% and 8.1%, respectively. The uncertainties in heat flux measurements are 15% at 16 kPa and 5.7% and at

3000 kPa of contact pressure. The uncertainty in temperature drop measurements are 0.25% at 16 kPa and 1.25% at 3000 kPa. Using the method described by Holman[9], the uncertainties of the thermal contact conductance measurements for SS 304 are ±15% at 16 kPa and ±4% at 3000 kPa. For Ni 200, the uncertainties are ±16% at 16 kPa and ±6% at 3000 kPa.

## EXPERIMENTAL RESULTS AND COMPARISON WITH THEORY

The mechanical and thermal properties and roughness parameters of the test specimens as well as the range of other test parameters are presented in Table 2. The tests are named here with a letter followed by a number: S1, S2, S3, N1, N2, and N3. The letter refers to the metal, "S" for SS 304 and "N" for Ni 200, and the numbers are related to the roughness of the pair tested: the rougher the pair, the larger the number, i. e., the N3 test specimens have total roughness $\sigma$ larger than the N2 test and so on.

The $\sigma$, $m$ and $\sigma/m$ values presented in this table are the average of the values obtained from the five profiles taken from each surface. The ratio $\sigma/m$ is commonly used as a measure of the roughness level of the surface; it is a better representation of the roughness level than $\sigma$ alone because $\sigma/m$ appears explicitly in the theoretical models, Eqs. (2), (3), (8), (10), (12) and (15).

The $c_1$ and $c_2$ values presented in Table 2 were obtained from five indentations for each load. The average of the ten diagonal lengths (two diagonals for each indentation) and the average of the five hardness values for each indentation were used to obtain the correlation coefficients according to Eq. (13). The range of the apparent contact pressures $P$, mean interface temperature $T_m$, temperature drop $\Delta T$ and heat flux at the interface $q$, as well as the thermal conductivity at the interface $k$, computed as a function of $T_m$ according to Eqs. (21) and (22), are also presented in Table 2.

The values of $z_{trunc}$ presented in Table 2 were obtained by fitting the correlation of the TG thermal contact conductance model for plastic deformation during the first loading, Eqs. (10) and (11) to the experimental data points. Figure 2 illustrates this procedure. For the case presented in Fig. 2 (test S3), the TG model with a value of $z_{trunc} = 3.5$ gives a line that is parallel to the data points, therefore $z_{trunc} = 3.5$ is adopted as the truncation level in this case. The data points do not have to lie exactly over the best line. Instead, the best line is the one which is parallel to the data points. As discussed extensively by Milanez et al.[4] and it will be addressed later on; this is believed to be the only accurate method to estimate $z_{trunc}$.

**Table 2** – Mechanical, thermal, geometrical and other test parameters

| parameter\test | S1 | S2 | S3 | N1 | N2 | N3 |
|---|---|---|---|---|---|---|
| $\sigma/m$ [μm] (total) | 17.7 | 26.2 | 40.0 | 23.0 | 27.0 | 48.0 |
| $\sigma$ [μm] (bead blasted) | 0.7 | 1.3 | 3.9 | 1.7 | 3.0 | 4.2 |
| $m$ (bead blasted) | 0.036 | 0.047 | 0.098 | 0.074 | 0.11 | 0.086 |
| $\sigma$ [μm] (lapped) | 0.12 | 0.12 | 0.12 | 0.10 | 0.10 | 0.10 |
| $m$ (lapped) | 0.022 | 0.022 | 0.022 | 0.017 | 0.017 | 0.017 |
| total flatness dev. [μm] | 0.9 | 0.8 | 0.7 | 0.6 | 0.6 | 0.6 |
| $c_1$ [GPa] | 10.67 | 10.67 | 10.67 | 4.33 | 4.33 | 4.33 |
| $c_2$ [ - ] | -0.37 | -0.37 | -0.37 | -0.079 | -0.079 | -0.079 |
| $z_{trunc}$ | 4.1 | 3.8 | 3.5 | 4.2 | 4.2 | 3.9 |
| $k$ [W/m·K] | 18.4 to 19.5 | 18.3 to 19.4 | 18.2 to 19.2 | 84.2 to 87.3 | 84.8 to 87.3 | 85.8 to 87.0 |
| $P$ [kPa] | 15.8 to 2,768 | 15.8 to 2,720 | 15.8 to 3,450 | 16.2 to 1,970 | 16.2 to 1,780 | 16.2 to 2,080 |
| $H_c$ [GPa] | 6.2 to 3.8 | 6.6 to 3.3 | 6.5 to 2.7 | 3.7 to 3.4 | 3.6 to 3.4 | 3.6 to 3.2 |
| $T_m$ [°C] | 23 to 65 | 20 to 63 | 19 to 54 | 16 to 33 | 16 to 30 | 17.5 to 24 |
| $\Delta T$ [°C] | 5.5 to 48 | 7 to 85 | 9 to 77 | 9 to 21 | 9 to 19 | 9 to 19 |
| $q$ [W/m$^2$] | 290 to 19,000 | 365 to 12,000 | 280 to 7,980 | 1,200 to 35,500 | 1,200 to 41,200 | 280 to 7,980 |

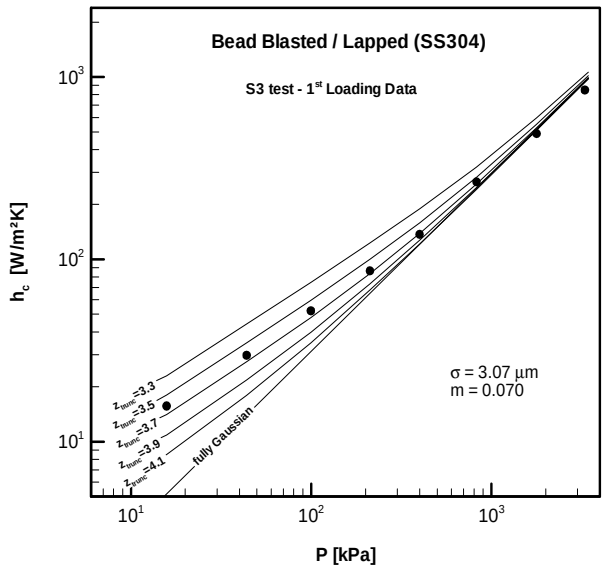


**Figure 2** – First-loading data from S3 test and comparison with the TG model for various values of $z_{trunc}$

Figures 3 to 5 show plots of $h_c$ against $P$ for SS 304 for the three roughness levels tested. Figures 6 to 8 present the results for the Ni 200 tests. The experimental data, as well as the theoretical models for first loading and unloading are presented. For first loading, the CMY plastic model with the fully Gaussian geometry model is presented as a dashed line and the CMY plastic model with the TG geometry model is presented as a continuous line. For unloading, the Mikic[2] fully Gaussian model is presented as a dotted line and the Mikic[2] model adapted according to the TG geometry model is presented as a dash-dotted line. The black squares are the first-loading experimental data, while the white squares are the first-unloading data. The black circles are the second-loading data and the white circles are the second-unloading data points.

In general, the results are practically the same for both metals and all roughness levels tested. The first-unloading data points lie above the first-loading data points, which characterizes the hysteresis effect of thermal contact conductance. That is an indication that plastic deformation took place during the first loading. In general, the hysteresis effect is negligible during the first-unloading/second-loading/second-unloading process, indicating the appearance of elastic deformation. These observations are in agreement with the theory described by Mikic[2].

The fully Gaussian model underpredicts the first-loading data at light loads. As the contact pressure increases, the model tends to the measured values. The TG first-loading model with apropriate values of $z_{trunc}$ predicts the data points over the entire range very well.

Both unloading models (fully Gaussian and TG) predicted the experimental data fairly well for contact pressure larger than 300 kPa. For $P < 300$ kPa, the fully Gaussian unloading model predicted the data better than the TG unloading model, although the TG unloading model predicted the trend of data points better than the fully Gaussian unloading model.

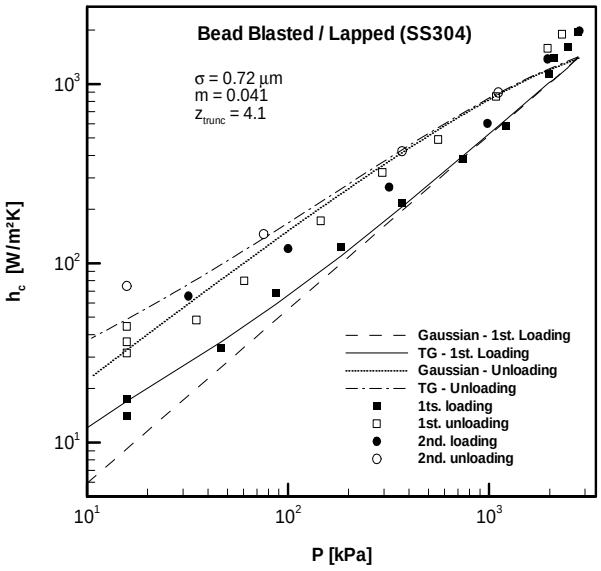


**Figure 3** – Results from test S1

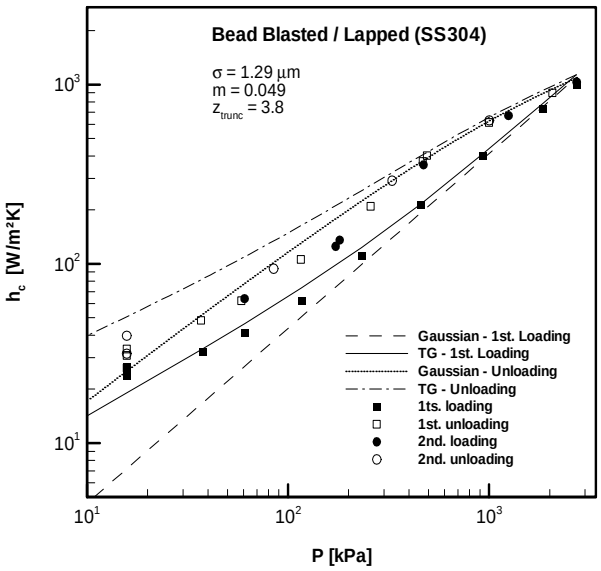


**Figure 4** – Results from test S2

Table 3 ilustrates the improvement in the agreement between theory and experiments when one uses the TG model instead of the fully Gaussian geometry model. This table shows the RMS differences between the measured and the predicted values of thermal contact conductance during first loading according to the fully Gaussian and the TG models. As one can see, the differences for the TG model are between 5.4 and 17.5%, while the differences for the fully Gaussian model are between 21.1 and 48.4%.

Truncation levels of bead blasted surfaces

As seen in Table 2, the $z_{trunc}$ values that make the model fit to the SS 304 data are 4.1, 3.8 and 3.5 for $\sigma/m$ values of 17.7, 26.2 and 40.0, respectively. For Ni 200, the $z_{trunc}$ values are 4.2, 4.2 and 3.9 for $\sigma/m$ values of 23.0, 27.0 and 48.0, respectively. The $z_{trunc}$ values that promote the better fitting between the TG model and the first-loading data points decrease with the roughness level $\sigma/m$. The values of $z_{trunc}$ for Ni 200 are larger than the values for the SS 304 tests, indicating that the bead blasting process is able to generate high asperities more likely for Ni 200 than for SS 304, despite the latter have a slightly smaller bulk hardness than the former (approximately 1500 MPa for SS 304 against 1700 MPa for Ni 200).

The values of $z_{trunc}$ presented in Table 2 can be used as a reference for the truncation levels of bead blasted SS 304 and Ni 200 surfaces. They can also be used to estimate the truncation levels of bead blasted SS 304 and Ni 200 for values of $\sigma/m$ other than those tested here by means of linear interpolation. However, it would be very useful if one could measure $z_{trunc}$ directly from surface profilometry, using the same equipment employed to measure the other roughenss parameters $\sigma$ and $m$. That would be specially helpful in order to measure the $z_{trunc}$ values for other metals and other surface machining processes, since the values presented here are valid only for Ni 200 and SS 304 prepared by bead blasting. Unfortunately, it seems like that is not case, as discussed extensively by Milanez et al.[4] and will be briefly reviewed here.

The stylus profilometer is the most common equipment employed for surface roughness measurement. It consists basically of a sharp diamond stylus which is dragged over the surface. As the stylus passes over the asperities that constitute the surface, it moves up and down and the vertical displacements are measured. At the end of the process, the equipment is able to measure a profile of the surface. The surface profile height measurements are then converted into roughness parameters such as $\sigma$ and $m$.

Most of the commercially available stylus profilometers measure another surface roughness parameter, generaly called $R_p$, which is the height of the highest asperity of the profile. The objective now is to compare the $z_{trunc}$ values available from thermal tests with $R_p$ measurements. Since $z_{trunc}$ is the truncation level normalized by the RMS roughness $\sigma$, $R_p$ must be divided by $\sigma$ also. Figure 9 presents 136 $R_p/\sigma$ measurements collected from 24 bead blasted SS 304 surfaces generated at several roughness levels. As one can see, the points are distributed over a very wide area. In general, for the same roughness level, the measured values of $R_p/\sigma$ are spread between 2.5 and 4.5. Rupert[10] conducted a similar study on surfaces prepared by turning, lapping and grinding and made similar observations. As ilustrated in Fig. 2, the TG model is very sensitive to the value of $z_{trunc}$. At the lightest contact pressure presented in Fig. 2 (15.8 kPa), for a variation of $z_{trunc}$ from 4.1 to 3.3, the model varies from approximately 8 to 20 W/m$^2$K, i. e., a 150 % difference. Given the large variation of $R_p/\sigma$ values, it is difficult to say which one is the best estimation of $z_{trunc}$. Therefore, one can conclude that $R_p/\sigma$ values obtained from ordinary profilometry are not accurate to estimate $z_{trunc}$. One must instead rely on the values of $z_{trunc}$ obtained by fitting the TG model to thermal data in order to predict accurately the effect of surface roughness truncation on contact conductance. The values obtained in this work for bead blasted SS 304 and Ni 200 can be used to estimate $z_{trunc}$ for these metals provided the surfaces are prepared by bead blasting. For other metals and other surface preparation methods, new tests are needed.

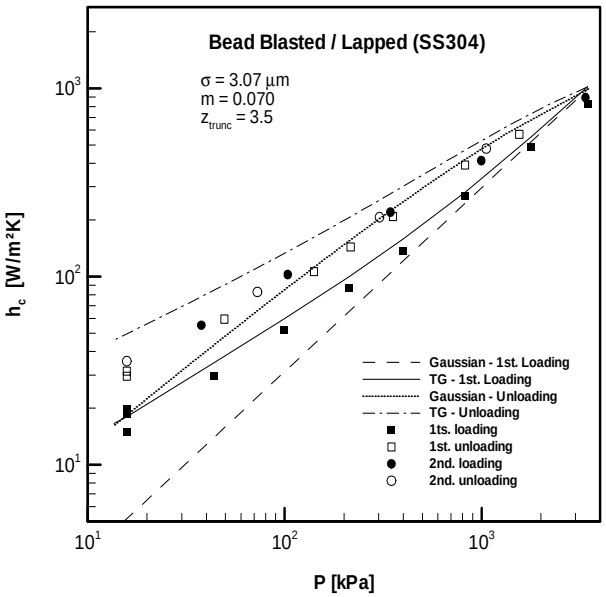


**Figure 5** – Results from test S3

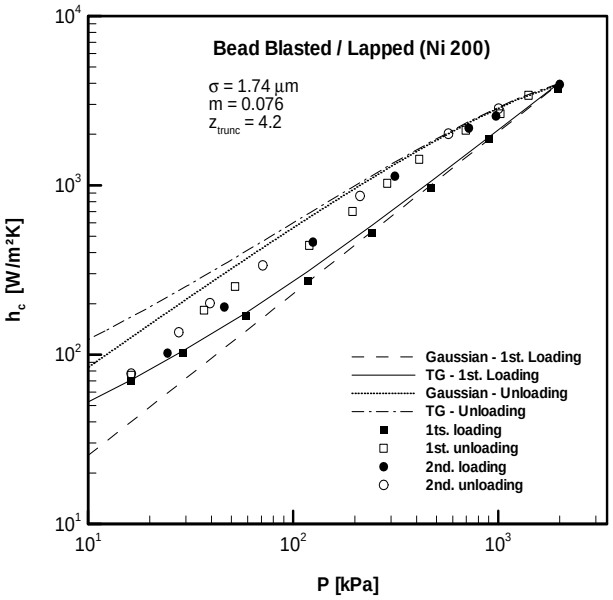


**Figure 6** – Results from test N1

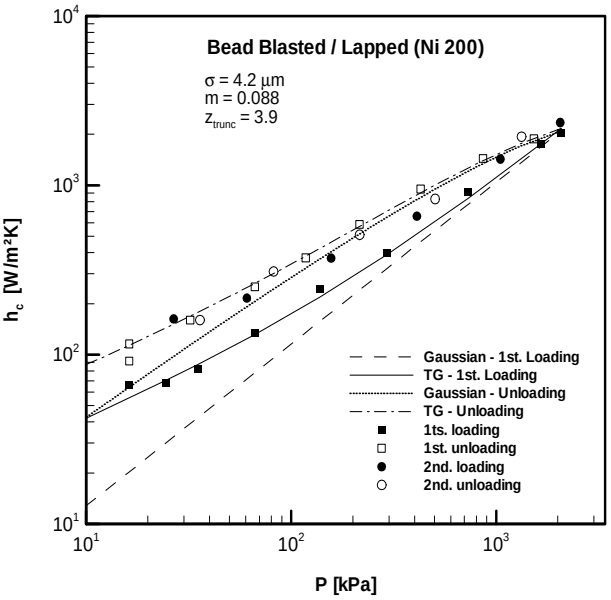


**Figure 8** – Results from test N3

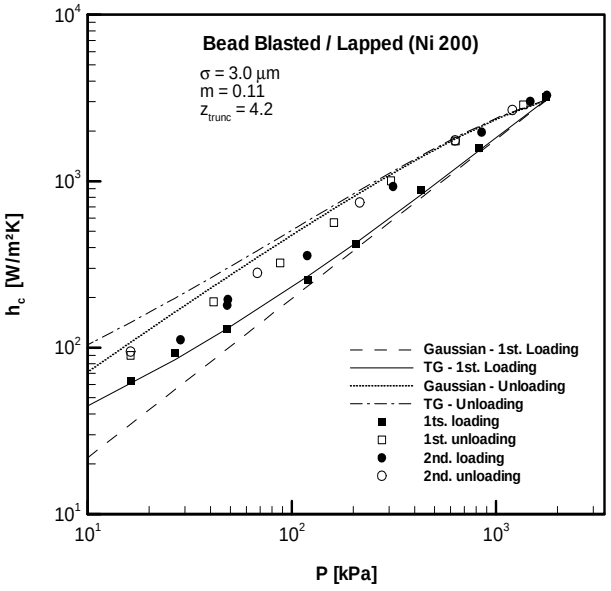


**Figure 7** – Results from test N2

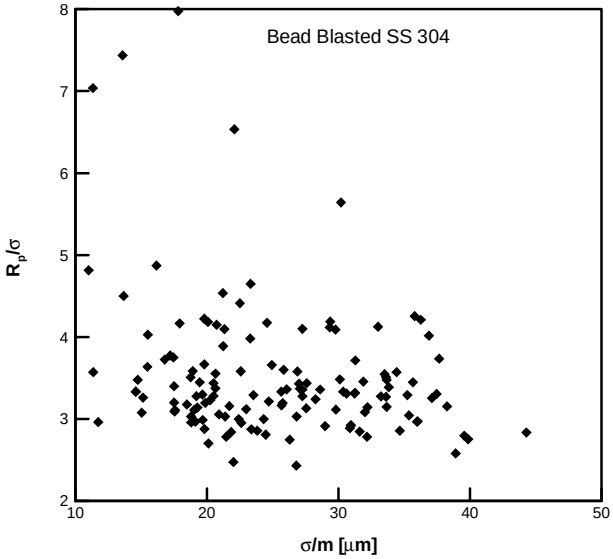


**Figure 9** - $R_p/\sigma$ versus $\sigma/m$ for bead blasted SS 304 surfaces

**Table 3** – RMS differences between the first-loading data and the models

| | RMS Difference [%] | | | | | | |
|---|---|---|---|---|---|---|---|
| | **Test** | **S1** | **S2** | **S3** | **N1** | **N2** | **N3** |
| *First-loading model* | **Gaussian** | 25.3 | 44.1 | 48.4 | 21.1 | 25.1 | 41.2 |
| | **TG** | 16.1 | 17.5 | 15.6 | 8.2 | 5.4 | 8.4 |

## SUMMARY AND CONCLUSIONS

This work presents new correlations for the TG thermal contact conductance model proposed by Milanez et al.[4] for first loading. Adaptations to the Mikic[2] unloading model and to the Song and Yovanovich[6] plastic contact pressure model according to the truncated Gaussian geometry model are also presented here. The models are compared against new thermal contact conductance data collected at very low contact pressures. The comparison between the models and the data show that the first-loading, fully Gaussian, model underpredicts data at low contact pressures, as already extensively reported in the literature. The first-loading TG model predicts the experiments very well over the entire range of the contact pressures tested. The Mikic[2] unloading model proved to be accurate only for contact pressure above 400 kPa, in general.

The TG model requires an extra surface roughness parameter, the level of truncation of the probability density function of surface heights ($z_{trunc}$). Unfortunately, this surface roughness parameter can not be accurately determined from ordinary surface profilometry. The most accurate and straightforward way to estimate $z_{trunc}$ is from thermal tests. This procedure consists of measuring thermal contact conductance for several contact pressure levels in the low contact pressure range (less than 700 kPa) and then comparing the data with the TG model for several values of $z_{trunc}$. The value of $z_{trunc}$ that leads to the best fit between the TG model and the data is the truncation level of the surface height distribution. In this work, truncation levels for bead blasted SS 304 and Ni 200 for various roughness levels are presented. These values can be used as a reference to predict the truncation levels of bead blasted SS 304 and Ni 200. New tests are needed for other metals and other surface machining processes.

## ACKNOWLEDGEMENTS

The first and the third authors would like to acknowledge the Brazilian Federal Agency for Post-Graduate Education-CAPES for providing the scholarship and the Brazilian Space Agency for supporting this project. The second author would also like to acknowledge the financial support of the Natural Sciences and Engineering Research Council of Canada.

## REFERENCES

[1]Cooper, M., Mikic, B. B. and Yovanovich, M. M., "Thermal Contact Conductance," *Journal of Heat and Mass Transfer*, Vol.12, pp. 279-300, 1969.

[2]Mikic, B. B., "Analytical Studies of Contact of Nominally Flat Surfaces: Effect of Previous Loading," *Journal of Lubrication Technology*, pp. 451-456, October, 1971.

[3]Sridhar, M. R. and Yovanovich, M. M., "Review of Elastic and Plastic Contact Conductance Models: Comparison with Experiment," *Journal of Thermophysics and Heat Transfer*, Vol. 8, No. 4, pp. 633-640, Oct.-Dec., 1994.

[4]Milanez, F. H., Yovanovich, M. M. and Culham, J. R., "Effect of Surface Asperity Truncation on Thermal Contact Conductance," *VIII Itherm*, May 29 - June 1, San Diego, CA, 2002.

[5]Song, S. "Analytical and Experimental Study of Heat Transfer through Gas Layers of Contact Interfaces," Ph. D. Thesis, Department of Mechanical Engineering, University of Waterloo, Waterloo, Ontario, Canada, 1988.

[6]Song, S. and Yovanovich, M. M., "Relative Contact Pressure: Dependence on Surface Roughness and Vickers Microhardness," *Journal of Thermophysics and Heat Transfer*, Vol. 2, No. 4, pp. 633-640, 1988.

[7]Yovanovich, M. M., "Thermal Contact Correlations," *Spacecraft Radiative Heat Transfer and Temperature Control*, Edited by T. E. Horton, Progress in Astronautics and Aeronautics, Vol. 83, NY, 1981.

[8]Journal of Physical and Chemical Reference Data, Vol. 3, Supplement No. 1, 1974.

[9]Holman, J. P., *Experimental Methods for Engineers*, 6th Edition, McGraw-Hill, Singapore, pp. 49-103, 1994.

[10]Rupert, M. P. "Confusion in Measuring Surface Roughness," *Engineering*, October 23, pp. 393-395, 1959.